



ARTICLE

Study on the Tangential Tensile Mechanical Properties of Moso Bamboo

Biqing Shu^{1,2}, Lu Hong³, Suxia Li^{1,4}, Yupeng Tao², Jianxin Cui¹, Naiqiang Fu², Junbao Yu², Chen Li² and Xiaoning Lu^{1,*}

¹The College of Materials Science and Engineering, Nanjing Forestry University, Nanjing, 210037, China

²College of Civil Engineering, Yangzhou Polytechnic Institute, Yangzhou, 225127, China

³School of Forestry and Landscape, Anhui Agricultural University, Hefei, 230036, China

⁴College of Furniture and Art Design, Central South University of Forestry and Technology, Changsha, 410004, China

*Corresponding Author: Xiaoning Lu. Email: luxiaoning-nfu@126.com

Received: 21 October 2021 Accepted: 30 November 2021

ABSTRACT

In this work, we used tensile tests to analyze the tangential failure forms of raw bamboo and determine a relationship between tangential tensile strength, elastic modulus, position, density, and moisture content. We found that the tangential mechanical properties of the culm wall were mainly dependent on the mechanical properties of the basic structure of the thin wall. Formulas for calculating the tangential tensile strength of moso bamboo and adjusting the moisture content were also determined. The tangential tensile strength and the tangential tensile modulus of elasticity (TTMOE) followed: outer > middle > inner, and diaphragm > bamboo node > culm wall. Below the fiber saturation point, the tangential tensile strength and TTMOE values of the bamboo gradually decreased with increasing moisture content. When the moisture content was 15%, the tangential tensile strengths of the inner, middle, outer, culm wall, bamboo node, and diaphragm samples of the five-year-old moso bamboo were 3.17, 3.29, 3.31, 3.24, 3.67, and 8.85 MPa, respectively. Furthermore, their TTMOE values were 215.09, 227.98, 238.45, 224.04, 267.21, and 559.27 MPa, respectively. Hence, this study provides a theoretical basis for future research on bamboo cracking.

KEYWORDS

Engineering raw bamboo; moso bamboo; tangential tensile strength; tangential tensile modulus of elasticity; bamboo cracking

1 Introduction

Large-diameter moso bamboo (*Phyllostachys edulis*) tubes are used as the main force-bearing members in construction projects for forming engineering raw bamboo, while small-diameter moso bamboo and its branches are used in fiberboard manufacturing [1,2]. Using raw bamboo in construction projects can reduce the energy consumption of bamboo processing; however, moso bamboo can easily crack during storage, transportation, and after felling [3]. Once the raw bamboo is cracked, it will cause the bamboo to rot, which and reduces its strength.

Bamboo loses water due to the equilibrium moisture content of the external environment and consequently, shrinks and deforms; therefore, cracks will easily occur in raw bamboo when the tensile



stresses on its inner and outer surfaces exceed the tangential tensile strength. Hence, the tangential tensile strength and the TTMOE play vital roles in moso bamboo cracking.

Extensive research has been conducted to analyze the longitudinal tensile strength, compressive strength, flexural strength, stiffness, and elastic modulus of bamboo along the fiber direction. However, the radial and tangential mechanical properties of bamboo have rarely been explored [3].

Bamboo exhibits better mechanical properties than ordinary wood and has excellent compression and bending resistance [4,5]. Bamboo fracture is characterized by three forms: matrix failure, interface dissociation and fiber fracture [6]. Moisture content has a significant effect on the mechanical properties of bamboo, and bamboo with high moisture content has higher fracture energy. According to Askarnejad et al. [7], the high strength of moso bamboo is due to the vascular bundle fibers that can withstand high stress during deformation. Bamboo nodes and vascular bundles mainly affect the energy absorption capacity of bamboo, and the energy absorption capacity of the nodes is greater than that of internodes [8]. Tian et al. Calculated the knotted and parallel grain tensile strength of moso bamboo as 163.1 MPa, with a non-knotted tensile strength along the grain of 177.9 MPa, and along the grain tensile modulus of elasticity of 11.65 GPa [9]. The compressive strength of Moso bamboo was calculated as 45–65 N/mm² [10]. In addition section, the compressive strength of upper bamboo section will be higher than that of the bottom, which is caused by more vascular bundles in the upper part of bamboo. From the inner layer to the outer layer, the strength and stiffness of bamboo gradually increase, and the bamboo with high bamboo stem has higher mechanical properties [11,12]. The average strength of bamboo is similar to that of hardwood. Compared with the outside, bamboo has higher toughness and lower hardness [13,14]. The tensile, compressive and flexural strength of bamboo decreased significantly with the increase of humidity. Askarnejad et al. observed the highest bamboo shear modulus of bamboo at 60% humidity and the highest bamboo shear strength at 60%–80% humidity [15]. Thus, bamboo becomes more ductile as humidity increases. The properties of fiber also have a significant impact on the properties of bamboo. The tensile strength of bamboo decreases with the increase of fiber diameter, and the fatigue life and fatigue limit increase with the decrease of fiber density [16,17]. Furthermore, Akinbade et al. observed that the bending strength and stiffness of bamboo stems are greatly affected by the silica rich epidermal layer, which is attributed to the destruction of the parenchyma near the outer stem wall at the interface between parenchyma cells [18].

Mo et al. [19] performed rapid hot pressing on four six-year-old moso bamboo slices at high temperatures and obtained calculated compressive strengths of 63.78–80.19 MPa, flexural strengths of 61.85–151.00 MPa, and flexural elastic modulus values of 7071.14–10487.44 MPa. Kadivar et al. [20] used an open hot press to densify the bamboo and noticed that bamboo had the best bending performance when the moisture content was 10%, with average calculated bamboo static bending strength, elastic modulus, and dynamic elastic modulus values of 318, 27754, and 34120 MPa, respectively.

The GB/T15780-1995 (Testing methods for the physical and mechanical properties of bamboo) and JG/T199-2007 (Testing methods for the physical and mechanical properties of bamboo used in buildings) standards do not have regulations for assessing the tangential tensile strength of raw bamboo. According to these two standards, the length of a tensile strength test piece must be at least 280 mm along the grain direction, and for the GB/T14017-2009 standard (Method of testing in tensile strength perpendicular to grains of wood), the length of the horizontal grain must be 150 mm. However, moso bamboo does not typically have a sufficient tangential length of 150 mm; thus, the tangential tensile strength of moso bamboo is rarely studied.

Zeng et al. [21] calculated the internode transverse grain tensile strength of moso bamboo as 3.0 ± 0.96 MPa and the transverse grain tensile strength at the nodes as 3.6 ± 0.85 MPa. However, the specimen dimensions used for the anti-splitting tests were not clearly defined, and the tangential tensile strengths of

tangential direction. Because the additional bending moment decreases the actual detected values, the effect of the additional bending moment was ignored. The cross-sections and dimensions of the inner, middle, outer, culm wall, bamboo node, and diaphragm specimens are shown in Fig. 2.

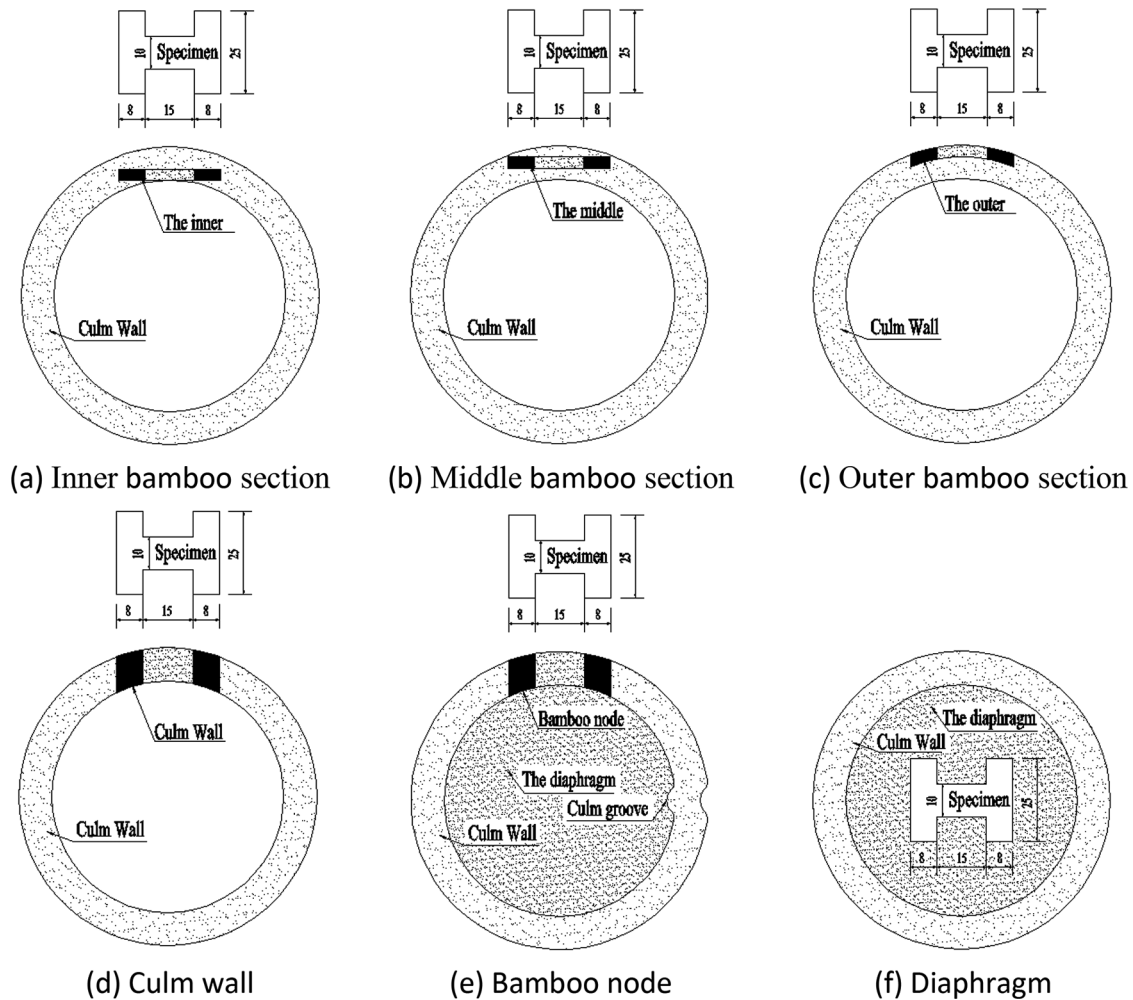


Figure 2: Cross-sections and dimensions (in mm) of the different test pieces. (a) Inner bamboo section (b) Middle bamboo section (c) Outer bamboo section (d) Culm wall (e) Bamboo node (f) Diaphragm

The moso bamboo was first cut into 25-mm-long bamboo rings using a sliding table saw. The bamboo rings were then cut into 25 mm × 31 mm bamboo blocks using a micro band saw machine, and the obtained bamboo blocks were finally cut into the inner, the middle, and the outer specimens with a small sliding table saw. The specimens were then polished to corresponding thicknesses with a sanding machine and milled to the sizes shown in Fig. 2 using a micro bench drilling and milling machine.

The two opposite sides of the effective cross-sections of each test piece were flat and parallel to each other. The test pieces also had no defects and were numbered randomly after processing. The allowable deviations for specimen length, width, and effective width were ± 1.0 mm, ± 0.5 mm, and ± 0.2 mm, respectively.

2.1.3 Specimen Storage and pre-Treatment

After processing, the bamboo test pieces were placed in a cool and ventilated place without stacking so that they could freely release water.

The test pieces were then placed in an HWS-250 constant temperature and humidity box before the experiment, and their moisture content values were adjusted to 5%, 10%, 15%, and 20% to obtain the four different sample sets.

2.2 Experimental Devices

In this experiment, we used the following equipment: a D-54518 Niersbach sliding table saw, an MBS240/E mini band saw machine, a No. 27070 mini sliding table saw, an MF70 mini bench drilling and milling machine (PROXXON Co., Ltd., Germany), a LUXTER-MM491G sand tray machine (Jinhua Maituo Power Tools Co., Ltd., China), an HWS-250 constant temperature and humidity box (Shanghai Jinghong Experimental Equipment Co., Ltd., China), a BS423S electronic balance (Shanghai Meiyongpu Instrument Manufacturing Co., Ltd., China), a WDW-200 electronic universal testing machine (Changchun Xinte Testing Machine Co., Ltd., China), and 150 T vernier calipers (Shanghai Menet Industrial Co., Ltd., China).

2.3 Evaluation Criteria

The bamboo fibers were naturally dried and finely ground after steam explosion, and their sieving value was determined with a Bauer-McNett fiber sieving instrument according to the TAPPI T233 method.

The bamboo specimens were tested at $20 \pm 2^\circ\text{C}$ with $65 \pm 5\%$ relative humidity. Each specimen was clamped with a clamping device and placed vertically in the tensile testing machine, and the stress (σ), strain (ε), and maximum load (F_{max}) of the specimens were automatically recorded by a computer.

The tangential tensile strengths (f_{tw}) of the specimens were calculated by

$$f_{tw} = F_{max}/(bt)$$

where b and t are the width and thickness of the effective portion of the specimens, respectively. The total dry densities (ρ_0) of the specimens were calculated by

$$\rho_0 = m_0/V_0$$

where m_0 and V_0 are the total dry mass and total dry volume of the specimens, respectively.

Linear numerical fitting was performed on automatically recorded stress and strain values to fit a straight line $\sigma = E\varepsilon + a$ (a is an arbitrary constant and E is the TTMOE), on the basis of a significance level of $R^2 \geq 0.90$.

2.4 Data Processing Methods

To analyze the rules of the test data, we obtained the standard deviations for each data group and checked whether the number of test pieces in each group met the requirements. In this study, we calculated the relevant statistics in accordance with JG/T199-2007.

3 Results and Discussion

3.1 Bamboo Tangential Failure Mode

The failure modes of each specimen are shown in Fig. 3. Fig. 3a shows that hard marrow ring tissue with highly woody fossil cells was present in the inner bamboo specimen. Moreover, no vascular bundle distribution was detected, causing the broken surface of the inner specimen to be inclined and irregular.

As shown in Figs. 3b–3e, the damaged surfaces of the middle, outer, culm wall, and bamboo node specimens were parallel to the fiber bundles.

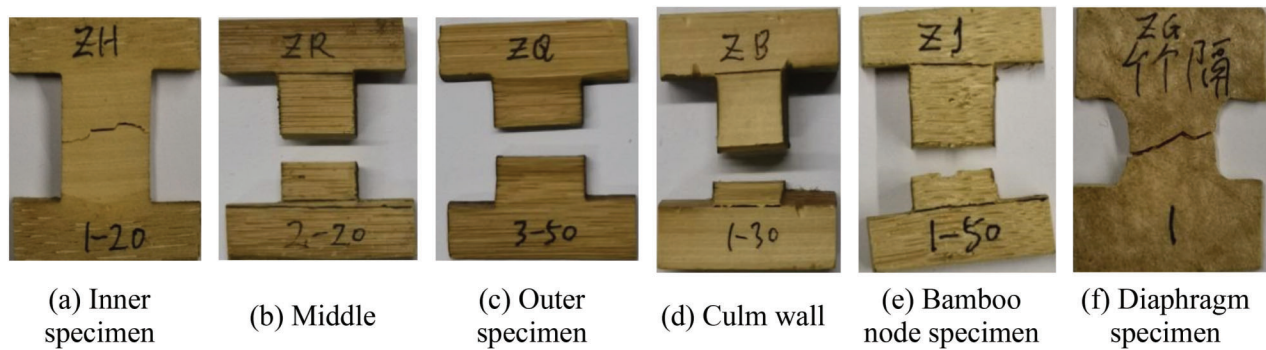


Figure 3: Failure modes of the different bamboo specimens. (a) Inner specimen (b) Middle Specimen (c) Outer specimen (d) Culm wall Specimen (e) Bamboo node specimen (f) Diaphragm specimen

As shown in Fig. 3f, the section failure surface of the diaphragm had an irregular slope. Reticular vascular bundles of the segment formed from the centripetal bending, bifurcation, merging, radiating extension, winding, and staggering of the longitudinal vascular bundles at the bamboo nodes. The vascular bundles also gradually became denser and thicker from the middle section to the edges.

According to Chen et al. [24], bamboo has three fracture modes: matrix (multi-walled parenchyma cells) destruction, interfacial (fiber and fiber or fiber and parenchyma cells) dissociation, and fiber fracture.

We found that the tangential fracture of the culm wall mainly occurred due to matrix failure, which was accompanied by a small amount of interfacial dissociation (Fig. 4). In addition, the bamboo had no horizontal organization. Therefore, the tangential mechanical properties of the culm wall were mainly dependent on the mechanical properties of the thin-walled basic structure. The tangential strength in bamboo is provided by lignin, which acts as a glue, and the lignin in the thin-walled basic structure is responsible for cementation and determines the tangential strength of the material.

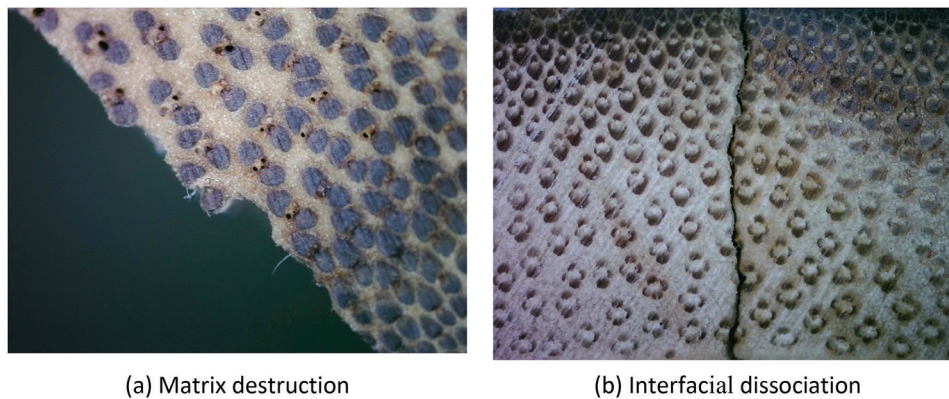


Figure 4: Choral fractures in the moso bamboo. (a) Matrix destruction (b) Interfacial dissociation

The formulas for calculating stresses at any point in a cross-section under the actions of a crack as follows:

$$\sigma_x = q \sqrt{\frac{a}{2r}} \cos \frac{\theta}{2} \left(1 - \sin \frac{\theta}{2} \sin \frac{3\theta}{2} \right) \quad (1a)$$

$$\sigma_y = q\sqrt{\frac{a}{2r}}\cos\frac{\theta}{2}\left(1 + \sin\frac{\theta}{2}\sin\frac{3\theta}{2}\right) \quad (1b)$$

$$t_{xy} = q\sqrt{\frac{a}{2r}}\sin\frac{\theta}{2}\cos\frac{\theta}{2}\cos\frac{3\theta}{2} \quad (1c)$$

where σ_x , σ_y , t_{xy} are the normal stress in the x direction, the normal stress in the y direction, and the shear stress at the crack endpoint, respectively, q is the tensile force, a is half of the original crack length, r is the distance from the calculation point to the crack endpoint, and θ is the angle between the line connecting the calculation point and the crack endpoint with the horizontal line.

As shown in formula (1), when $\theta = 0$, the σ_x and σ_y values were the largest. When the stress exceeds the chord tensile strength of the bamboo, cracking will occur; therefore, the crack propagation direction was along the thickness direction of the bamboo wall.

3.2 Tangential Tensile Strength

The tangential tensile strengths of the inner, the middle, outer, culm wall, bamboo node, and diaphragm specimens were measured with moisture content values of 5%, 10%, 15%, and 20%. We used eight test pieces for each group, according to article 6.5.3 of the JG/T199-2007 standard.

The tangential tensile strengths and related statistical data of the moso bamboo with moisture content values of 5%, 10%, 15%, and 20% are presented in Tables 1–4, respectively.

Table 1: Tangential tensile strengths of the moso bamboo with 5% moisture content

Location	Average value (MPa)	Standard deviation (MPa)	Mean standard deviation (MPa)	Accuracy index (%)	Minimum number of test pieces (piece)
Inner	4.42	0.99	0.35	15.84	6
Middle	4.57	0.93	0.33	14.39	7
Outer	4.63	0.95	0.34	14.51	7
Culm wall	4.51	0.87	0.31	13.64	8
Bamboo node	4.88	1.22	0.43	17.68	5
The diaphragm	10.63	2.14	0.76	14.24	8

Table 2: Tangential tensile strengths of the moso bamboo with 10% moisture content

Location	Average value (MPa)	Standard deviation (MPa)	Mean standard deviation (MPa)	Accuracy index (%)	Minimum number of test pieces (piece)
Inner	3.82	0.85	0.30	15.73	6
Middle	3.91	0.78	0.28	14.11	8
Outer	3.95	0.84	0.30	15.04	7
Culm wall	3.86	0.80	0.28	14.66	7
Bamboo node	4.32	0.95	0.34	15.55	6
The diaphragm	9.04	1.80	0.64	14.11	8

Table 3: Tangential tensile strengths of the moso bamboo with 15% moisture content

Location	Average value (MPa)	Standard deviation (MPa)	Mean standard deviation (MPa)	Accuracy index (%)	Minimum number of test pieces (piece)
Inner	3.17	0.61	0.22	13.61	8
Middle	3.29	0.68	0.24	14.61	7
Outer	3.31	0.82	0.29	17.52	5
Culm wall	3.24	0.69	0.24	15.06	7
Bamboo node	3.67	0.71	0.25	13.68	8
The diaphragm	8.85	1.79	0.63	14.34	7

Table 4: Tangential tensile strength of moso bamboo with 20% moisture content

Location	Average value (MPa)	Standard deviation (MPa)	Mean standard deviation (MPa)	Accuracy index (%)	Minimum number of test pieces (piece)
Inner	2.62	0.62	0.22	16.73	5
Middle	2.68	0.59	0.21	15.57	6
Outer	2.73	0.71	0.25	18.39	5
Culm wall	2.65	0.56	0.20	14.97	7
Bamboo node	2.70	0.61	0.22	16.00	6
The diaphragm	6.76	1.37	0.48	14.29	8

Of note, the outer section of bamboo had the highest tangential tensile strength followed by the middle and the inner sections; however, the difference was not significant. The tangential tensile strength of the culm wall was similar to the middle section. This occurred because more thin-walled basic tissues and fewer vascular bundles were present in the inner bamboo section (tangential tensile strength damage mainly occurs in thin-walled basic tissues).

Moreover, the diaphragm had the highest tensile strength followed by the bamboo node and the internode culm wall. The vascular bundles in the bamboo nodes had different degrees of bending, bifurcation or merging, and inward winding, and the horizontal vascular bundles in the diaphragm were arranged irregularly in a network. The tangential failure of the diaphragm and bamboo node led to fiber damage, and the diaphragm broke relatively more fibers.

With 15% moisture content, the tangential tensile strength values of the inner, middle outer, culm wall, bamboo node, and diaphragm specimens of the five-year-old moso bamboo were 3.17, 3.29, 3.31, 3.24, 3.67, and 8.85 MPa, respectively.

We found that below the fiber saturation point, the tangential tensile strength of each moso bamboo section gradually decreased as the moisture content increased. This mainly occurred because bamboo is composed of lignin, cellulose, hemicellulose, and lignin, which acts as the glue. Lignin is affected by humidity, and the bonding performance will decrease as wettability increases. In addition, the flexibility of hemicellulose will increase after water exposure.

3.3 TTMOE

The TTMOE values of the inner, middle, outer, culm wall, bamboo node, and diaphragm specimens were measured with moisture content values of 5%, 10%, 15%, and 20%. Eight test pieces were used for each group, according to Article 6.5.3 of the JG/T199-2007 standard.

The TTMOE values and related statistical data of the moso bamboo with moisture content values of 5%, 10%, 15%, and 20% are presented in [Tables 5–8](#), respectively.

Table 5: TTMOE values of the moso bamboo with 5% moisture content

Location	Average value (MPa)	Standard deviation (MPa)	Mean standard deviation (MPa)	Accuracy index (%)	Minimum number of test pieces (piece)
Inner	301.52	60.33	21.33	14.15	8
Middle	312.83	67.08	23.72	15.16	7
Outer	318.47	72.24	25.54	16.04	6
Culm wall	306.45	60.17	21.27	13.88	8
Bamboo node	324.47	78.45	27.74	17.10	5
The diaphragm	636.32	124.22	43.92	13.80	8

Table 6: TTMOE values of moso bamboo with 10% moisture content

Location	Average value (MPa)	Standard deviation (MPa)	Mean standard deviation (MPa)	Accuracy index (%)	Minimum number of test pieces (Piece)
Inner	265.17	57.51	20.33	15.34	7
Middle	277.30	62.07	21.95	15.83	6
Outer	281.21	63.14	22.32	15.88	6
Culm wall	270.34	55.62	19.66	14.55	7
Bamboo node	292.46	58.83	20.80	14.22	8
The diaphragm	584.78	119.08	42.10	14.40	7

Table 7: TTMOE values of moso bamboo with 15% moisture content

Location	Average value (MPa)	Standard deviation (MPa)	Mean standard deviation (MPa)	Accuracy index (%)	Minimum number of test pieces (Piece)
Inner	215.09	41.36	14.62	13.60	8
Middle	227.98	46.47	16.43	14.41	7
Outer	238.45	50.90	18.00	15.09	7
Culm wall	224.04	43.03	15.21	13.58	8
Bamboo node	267.21	58.28	20.61	15.42	6
The diaphragm	559.27	107.52	38.01	13.59	8

Table 8: TTMOE values of moso bamboo with 20% moisture content

Location	Average value (MPa)	Standard deviation (MPa)	Mean standard deviation (MPa)	Accuracy index (%)	Minimum number of test pieces (piece)
Inner	190.26	44.09	15.59	16.39	6
Middle	204.87	39.15	13.84	13.51	8
Outer	210.71	45.33	16.03	15.21	7
Culm wall	196.42	38.45	13.59	13.84	8
Bamboo node	225.75	53.22	18.82	16.67	6
The diaphragm	524.44	99.75	35.27	13.45	8

We found that the outer bamboo specimens had the largest TTMOE values, followed by the middle and inner specimens. Moreover, the diaphragm specimen had the highest TTMOE value followed by the bamboo node and the internode culm wall specimens. Below the fiber saturation point, the TTMOE values of each moso bamboo section gradually decreased as the moisture content increased.

With 15% moisture content, the TTMOE values of the inner, middle, outer, culm wall, bamboo node, and diaphragm five-year-old moso bamboo specimens were 215.09, 227.98, 238.45, 224.04, 267.21, and 559.27 MPa, respectively.

3.4 Calculation Formula for Tangential Tensile Strength

A moisture content value of 15% was selected as the research basis. The tangential tensile strength of the five-year-old bamboo wall was calculated, and the tangential tensile strength (σ) and air-dry density (ρ) of each specimen were determined. We also used 100 test specimens, according to the GB/T15780-1995 standard.

The tangential mechanical properties of the bamboo wall are mainly dependent on the mechanical properties of the basic structure of the thin wall. Shao et al. [25] calculated the elastic modulus (E_0) and tensile strength (σ_0) of thin-walled basic moso bamboo tissues as 0.22 GPa and 19.42 MPa, respectively (the average air-dry density of the moso bamboo was $\rho_0 = 0.81 \text{ g/cm}^3$).

As shown in Fig. 5, the density ratio ρ/ρ_0 and stress ratio σ/σ_0 were taken as the abscissa and ordinate, respectively, and linear fitting was performed to obtain a formula to calculate the tangential tensile strength of moso bamboo.

As clearly shown in Fig. 5, the stress ratio σ/σ_0 increased with increasing density ratio ρ/ρ_0 . When ρ/ρ_0 was between 0.8 and 1.2, σ/σ_0 increased linearly; however, when ρ/ρ_0 was lower than 0.8 or higher than 1.2, the change rate of σ/σ_0 decreased significantly.

When $0.8 \leq \rho/\rho_0 \leq 1.2$, the stress ratio σ/σ_0 and the density ratio ρ/ρ_0 were linearly fitted to obtain the formula for tangential tensile strength at a moisture content of ω .

$$\sigma_\omega = \left(0.198 \frac{\rho}{\rho_0} - 0.027 \right) \sigma_0 \quad (2)$$

where σ_ω is the tangential tensile strength of the moso bamboo with a moisture content of ω , σ_0 is the tensile strength of the basic parenchyma of *Phyllostachys edulis*, ρ is the air-dry density of the bamboo wall with a moisture content of ω , and ρ_0 is the average air-dry density of the bamboo wall.

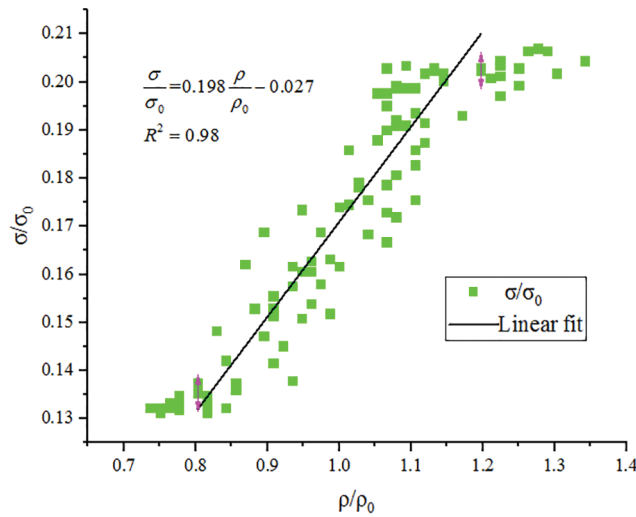


Figure 5: Calculation formula for the tangential tensile strength

3.5 Water Content Adjustment Formula for Tangential Tensile Strength

When the moisture content values were 5%, 10%, 15%, and 20%, the tangential tensile strength values of the bamboo wall were 4.51, 3.86, 3.24, and 2.65 MPa, respectively (Tables 1–4). Linear fitting was performed on these four sets of data to obtain a relationship curve between the bamboo tangential tensile strength and the moisture content, as shown in Fig. 6.

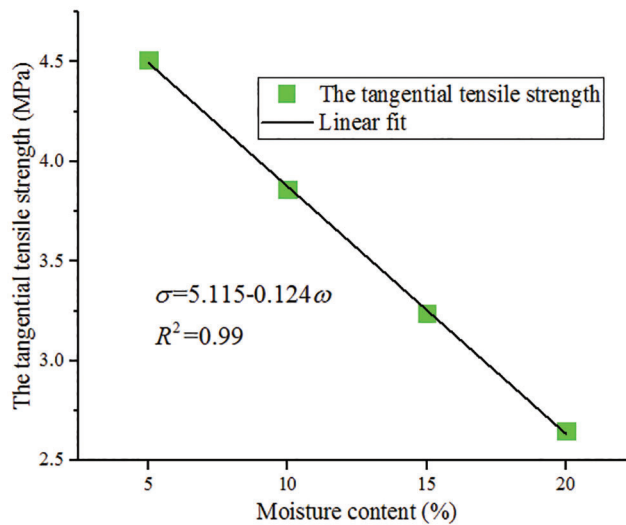


Figure 6: Relationship between the tangential tensile strength and the moisture content

The calculations fitted in Fig. 6 revealed that when the moisture content was 12%, the tangential tensile strength was 3.627 MPa.

The four tangential tensile strength groups with moisture content values of 5%, 10%, 15%, and 20% were divided by the tangential tensile strength, resulting in a moisture content value of 12%. These four sets of data were linearly fitted to obtain a relationship curve between the tangential tensile strength ratio and the moisture content, as shown in Fig. 7.

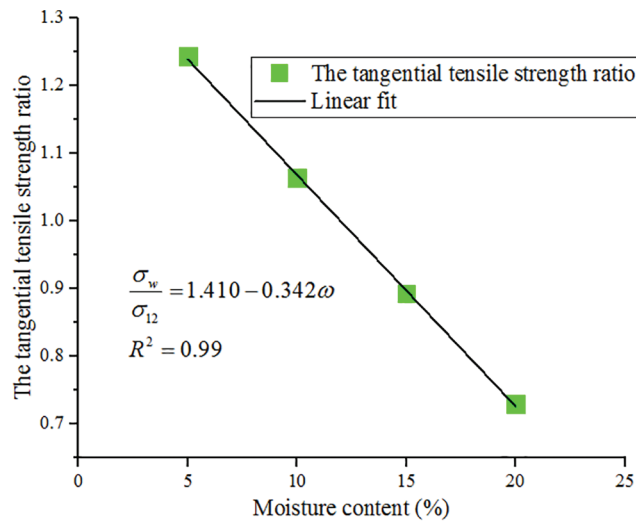


Figure 7: Relationship between the tangential tensile strength ratio and moisture content

Fig. 7 shows that when the moisture content was 12%, the moisture content adjustment formula for the tangential tensile strength of the moso bamboo could be formulated by:

$$\sigma_{12} = \frac{\sigma_{\omega}}{1 - 0.34(\omega - 12)} \quad (3)$$

where σ_{12} is the tangential tensile strength of the moso bamboo with 12% moisture content, and σ_{ω} is the tensile strength of the moso bamboo for a moisture content value of ω (where ω is the moisture content of the moso bamboo).

4 Conclusions and Recommendations

4.1 Conclusions

In this study, we conducted tangential tensile strength and TTMOE tests on five-year-old moso bamboo, and observed that the tangential mechanical properties of the culm walls were mainly dependent on the mechanical properties of the thin-walled basic structure.

Below the fiber saturation point, the tangential tensile strength and TTMOE values of all bamboo sections would gradually decrease with increasing moisture content. When the moisture content was 15%, the tangential tensile strength values of the inner, middle, outer, culm wall, bamboo node, and diaphragm five-year-old moso bamboo samples were 3.17, 3.29, 3.31, 3.24, 3.67, and 8.85 MPa, respectively, and their respective TTMOE values were 215.09, 227.98, 238.45, 224.04, 267.21, and 559.27 MPa.

Under the condition of $0.8 \leq \rho/\rho_0 \leq 1.2$, the formula for calculating the tangential tensile strength of bamboo with a moisture content of ω could be expressed by

$$\sigma_{\omega} = \left(0.198 \frac{\rho}{\rho_0} - 0.027 \right) \sigma_0$$

Thus, the moisture content adjustment formula $\sigma_{12} = \frac{\sigma_{\omega}}{1 - 0.34(\omega - 12)}$ could be used to adjust the tangential tensile strength of moso bamboo with different moisture content values, and for tangential strength with 12% moisture content.

4.2 Recommendations

In this study, moso bamboo samples were collected from Liyang City and Changzhou City of Jiangsu Province. In future research, moso bamboo samples will be collected from different regions, and the influence coefficient of moso bamboo performance in different regions will be used to adjust the formulas obtained through this analysis.

Acknowledgement: All authors contributed equally to this work.

Funding Statement: We thank the Sixth Phase of “333 Project” Training Objects in Jiangsu Province, Jiangsu Province High-Level Talent Selection Training (JNHB-127), the National Key R&D Program of China (2017YFC0703501), the National Natural Science Foundation of China (51878590), Jiangsu Provincial Department of Housing and Construction (2019ZD092, 2020ZD40 and 2020ZD42), the Natural Science Foundation of Jiangsu Province (Grant Nos. BK20170926, BK20150878 and 20KJB560010), and College Research Project (2019xjzk014) for funding this research.

Conflicts of Interest: The authors declare that they have no conflicts of interest to report regarding the present study.

References

1. Shu, B. Q., Ren, Q., He, Q., Ju, Z. H., Lu, X. N. et al. (2019). Study on mixed biomass binderless composite based on simulated wood. *Wood Research*, 64(6), 1023–1034.
2. Shu, B. Q., Ren, Q., Hong, L., Xiao, Z. P., Lu, X. N. et al. (2021). Effect of steam explosion technology main parameters on moso bamboo and poplar fiber. *Journal of Renewable Materials*, 9(3), 585–597. DOI 10.32604/jrm.2021.012932.
3. Shu, B. Q., Xiao, Z. P., Hong, L., Zhang, S. J., Lu, X. N. et al. (2020). Review on the application of bamboo-based materials in construction engineering. *Journal of Renewable Materials*, 8(10), 1215–1242. DOI 10.32604/jrm.2020.011263.
4. Chung, K. F., Yu, W. K. (2002). Mechanical properties of structural bamboo for bamboo scaffoldings. *Engineering Structures*, 24, 429–442. DOI 10.1016/S0141-0296(01)00110-9.
5. Gottron, J., Harries, K. A., Xu, Q. F. (2014). Creep behaviour of bamboo. *Construction and Building Materials*, 66, 79–88. DOI 10.1016/j.conbuildmat.2014.05.024.
6. Chen, G. W., Luo, H. Y., Yang, H. Y., Zhang, T., Li, S. J. (2018). Water effects on the deformation and fracture behaviors of the multi-scaled cellular fibrous bamboo. *Acta Biomaterialia*, 65, 203–215. DOI 10.1016/j.actbio.2017.10.005.
7. Askarinejad, S., Kotowski, P., Youssefian, S., Rahbar, N. (2016). Fracture and mixed-mode resistance curve behavior of bamboo. *Mechanics Research Communications*, 78, 79–85. DOI 10.1016/j.mechrescom.2016.02.001.
8. Zou, M., Wei, C. G., Li, J. Q., Xu, S. C., Zhang, X. (2015). The energy absorption of bamboo under dynamic axial loading. *Thin Walled Structures*, 95, 255–261. DOI 10.1016/j.tws.2015.06.017.
9. Tian, K. (2016). *Study on bending capacity of original bamboo-skeleton lightweight composite floor slab (Master Thesis)*. Xi'an University of Architecture and Technology, China.
10. Lo, T. Y., Cui, H. Z., Tang, P. W. C., Leung, H. C. (2008). Strength analysis of bamboo by microscopic investigation of bamboo fibre. *Construction and Building Materials*, 22, 1532–1535. DOI 10.1016/j.conbuildmat.2007.03.031.
11. Krause, J. Q., Silva, F. D. A., Ghavami, K., Gomes, O. D. F. M., Filho, R. D. T. (2016). On the influence of dendrocalamus giganteus bamboo microstructure on its mechanical behavior. *Construction and Building Materials*, 127, 199–209. DOI 10.1016/j.conbuildmat.2016.09.104.
12. Verma, C. S., Purohit, R., Rana, R. S., Mohit, H. (2017). Mechanical properties of bamboo laminates with other composites. *Materials Today:Proceedings*, 4, 3380–3386. DOI 10.1016/j.matpr.2017.02.226.

13. Mannan, S., Parameswaran, V., Basu, S. (2018). Stiffness and toughness gradation of bamboo from a damage tolerance perspective. *International Journal of Solids and Structures*, 143, 274–286. DOI 10.1016/j.ijsolstr.2018.03.018.
14. Jakovljević, S., Lisjak, D., Alar, Ž, Penava, F. (2017). The influence of humidity on mechanical properties of bamboo for bicycles. *Construction and Building Materials*, 150, 35–48. DOI 10.1016/j.conbuildmat.2017.05.189.
15. Askarinejad, S., Kotowski, P., Shalchy, F., Rahbar, N. (2015). Effects of humidity on shear behavior of bamboo. *Theoretical and Applied Mechanics Letters*, 5, 236–243. DOI 10.1016/j.taml.2015.11.007.
16. Monteiro, S. N., Margem, F. M., Braga, F. D. O., Luz, F. S. D., Simonassi, N. T. (2017). Weibull analysis of the tensile strength dependence with fiber diameter of giant bamboo. *Journal of Materials Research and Technology*, 6(4), 317–322. DOI 10.1016/j.jmrt.2017.07.001.
17. Song, J., James, U. S., Hu, D. Y., Lu, Y. (2017). Fatigue characterization of structural bamboo materials under flexural bending. *International Journal of Fatigue*, 100(1), 126–135. DOI 10.1016/j.ijfatigue.2017.03.016.
18. Akinbade, Y., Harries, K. A., Flower, C. V., Nettleship, I., Papadopoulos, C. et al. (2019). Through-culm wall mechanical behaviour of bamboo. *Construction and Building Materials*, 216, 485–495. DOI 10.1016/j.conbuildmat.2019.04.214.
19. Mo, J., Ma, Z. Q., Nie, Y. J., Ma, L. F. (2019). Physical and mechanical properties of phyllostachys edulis with fast hotpressing and high temperature. *Journal of Zhejiang A&F University*, 36(5), 974–980. DOI 10.11833/j.issn.2095-0756.2019.05.017.
20. Kadivar, M., Gauss, C., Mármol, G., Sá, A. D. D., Fioroni, C. et al. (2019). The influence of the initial moisture content on densification process of D. asper bamboo: physical-chemical and bending characterization. *Construction and Building Materials*, 229, 1–12. DOI 10.1016/j.conbuildmat.2019.116896.
21. Zeng, Q. Y., Li, S. H., Bao, X. R. (1992). Effect of bamboo nodal on mechanical properties of bamboo wood. *Scientia Silvae Sinicae*, 28(3), 247–252.
22. Zhong, S. (2011). *Preliminary study on the principle and protection of bamboo tubes' splitting (Master Thesis)*. Beijing Forestry University, China.
23. Guan, M. J., Zhu, Y. X., Mo, X. F., Mo, C. Z., Dong, D. Y. (2010). Performance on some basic physical properties of moso bamboo (*Phyllostachys pubescens*) during aging related to the selection of bamboo culms for green buildings. *Journal of Southwest University (Natural Science Edition)*, 32(1), 144–147. DOI 10.13718/j.cnki.xdzk.2010.01.025.
24. Chen, G. W., Luo, H. Y., Yang, H. Y., Zhang, T., Li, S. J. (2018). Water effects on the deformation and fracture behaviors of the multi-scaled cellular fibrous bamboo. *Acta Biomaterialia*, 65, 203–215. DOI 10.1016/j.actbio.2017.10.005.
25. Shao, Z. P., Fang, C. H., Huang, S. X., Tian, G. L. (2010). Tensile properties of moso bamboo (*Phyllostachys pubescens*) and its components with respect to its fiber-reinforced composite structure. *Wood Science & Technology*, 44(4), 655–666. DOI 10.1007/s00226-009-0290-1.